

Bayesian Approximations to Hidden Semi-Markov Models

Beniamino Hadj-Amar¹, Jack Jewson², and Mark Fiecas¹

¹*Division of Biostatistics, University of Minnesota*

²*Barcelona Graduate School of Economics, Unversitat Pompeu Fabra*

b.hadjama@umn.edu, jack.jewson@barcelonagse.eu, mfiecas@umn.edu

June 2020

Abstract

We propose a Bayesian hidden Markov model for analyzing time series and sequential data where a special structure of the transition probability matrix is embedded to model explicit-duration semi-Markovian dynamics. Our formulation allows for the development of highly flexible and interpretable models that can integrate available prior information on state durations while keeping a moderate computational cost to perform efficient posterior inference. We show the benefits of choosing a Bayesian approach over its frequentist counterpart, in terms of incorporation of prior information, quantification of uncertainty, model selection and out-of-sample forecasting. The use of our methodology is illustrated in an application relevant to e-Health, where we investigate rest-activity rhythms using telemetric activity data collected via a wearable sensing device.

Keywords: Markov Switching Process; Hamiltonian Monte Carlo; Bayes-Factor; Telemetric Activity Data;

1 Introduction

Recent developments in portable computing technology and the increased popularity of wearable and non-intrusive devices, e.g. smartwatches, bracelets, and smartphones, have provided exciting opportunities to measure and quantify physiological time series that are of interest in many applications, including mobile health monitoring, chronotherapeutic healthcare and cognitive behavioral treatment

of insomnia (Aung, Matthews, & Choudhury, 2017; Kaur, Phillips, Wong, & Saini, 2013; Silva, Rodrigues, de la Torre Díez, López-Coronado, & Saleem, 2015; Williams, Roth, Vathauer, & McCrae, 2013). The behavioral pattern of alternating sleep and wakefulness in humans can be investigated by measuring gross motor activity. Over the last twenty years, activity-based sleep-wake monitoring has acquired a remarkably central role as an assessment tool for quantifying the quality of sleep (Ancoli-Israel et al., 2003; Sadeh, 2011). Though polysomnography (Douglas, Thomas, & Jan, 1992), usually carried out within a hospital or at a sleep center, continues to remain the gold standard for diagnosing sleeping disorders, accelerometers have become a practical and inexpensive way to collect non-obtrusive and continuous measurements of restactivity rhythms over a multitude of days in the individuals home sleep environment (Ancoli-Israel et al., 2015).

Our study investigates the *physical activity* (PA) time-series first considered by Huang et al. (2018) and Hadj-Amar, Finkenstädt, Fiecas, Lévi, and Huckstepp (2019), where a wearable sensing device is fixed to the chest of a user to measure its movement via a triaxial accelerometer (ADXL345, Analog Devices). The tool produces PA counts, defined as the number of times an accelerometer undulation exceeds zero over a specified time interval. Figure 1 displays an example of 4 days of 5-min averaged PA recordings for a healthy subject, for a total of 1150 data points. Transcribing information from such complex, high frequency data into interpretable and meaningful statistics is a non-trivial challenge. There is a need for a data-driven procedure to automate the analysis of these types of measurements. Huang et al. (2018) addressed this task by proposing a hidden Markov model (HMM) within a frequentist framework. We formulate a more flexible approximate hidden semi-Markov model (HSMM) approach that enables us to explicitly model the dwell time spent in each state. Furthermore, our proposed modelling approach uses a Bayesian inference paradigm, allowing us to incorporate available prior information for different activity patterns and facilitate consistent and efficient model selection between dwell distribution.

In this paper we propose a Bayesian HMM that is a reformulation of any given HSMM. We utilise the method of Langrock and Zucchini (2011) to embed the generic state duration distribution within a special transition matrix structure that can approximate the underlying HSMM with arbitrary accuracy. This framework is able to incorporate the extra flexibility of explicitly modelling the state dwell-distribution provided by a HSMM, without renouncing the computational tractability, theoretical understanding and the multitudes of methodological advancements that are available when using an HMM. To the best of our knowledge, such a modeling approach have been treated only from a

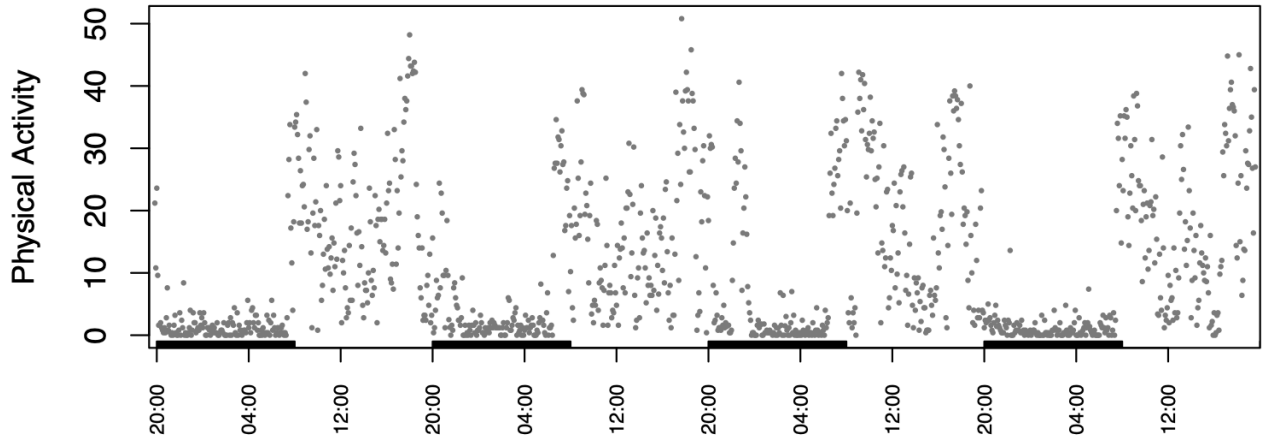


Figure 1: PA time series for a healthy individual. Rectangles on the time axis correspond to periods from 20.00 to 8.00.

non-Bayesian perspective in the literature, where parameters are estimated either by direct numerical likelihood maximization (MLE) or applying the expectation-maximization (EM) algorithm.

Rather than producing point estimates for the model parameters, our formulation is presented in a full Bayesian framework, where inference is carried out by treating the parameters as random variables and considering their *posterior* distributions. The posterior is computed using Bayes' rule, namely by combining the likelihood model with a *prior* distribution, the latter representing the beliefs about the parameter prior to analyzing the data. While the likelihood model is shared by both Bayesian and frequentist approaches, the concept of prior and posterior distributions for the model parameters is unique to the Bayesian paradigm. This results in Bayesian inference having two main practical advantages over its frequentist analogue: (i) the prior distribution allows a Bayesian analysis to incorporate practitioner expert judgements, regularizing the within-sample estimation and improving performance for short time series; (ii) the posterior distributions provides full uncertainty quantification for model parameters, automatically characterizing a full range of credibility sets and facilitating improved mechanisms for prediction and model selection. However, the posterior distribution is rarely available in closed form and the computational burden of approximating the posterior, often by sampling (see e.g. [Gelfand & Smith, 1990](#)), is considered as a major drawback of the Bayesian approach. In this paper we are able to leverage the probabilistic programming language *stan* ([Carpenter et al., 2016](#)) to produce fast and accurate samples from our posteriors. We take advantage of *stan*'s sparse

matrix implementation to further accelerate our inference and its compatibility with bridge-sampling (Gronau, Singmann, & Wagenmakers, 2020; Meng & Schilling, 2002; Meng & Wong, 1996) to facilitate Bayesian model selection.

The rest of this article is organized as follows. In Section 2.1, we provide a brief introduction on HMMs and HSMMs. Section 2.2 and 3 present the model and our formulation within a Bayesian framework as well as our inference approach. In Section 4, we investigate the performance of our proposed procedure in several simulation studies. Section 5 illustrates the use of our method to analyze telemetric activity data. The *stan* files (and R utilities) that were used to implement our experiments are available at <https://github.com/Beniamino92/BayesianApproxHSMM>.

2 Modeling Approach

2.1 Overview of Hidden Markov and Semi-Markov Models

We now provide a brief introduction on the standard HMM and HSMM approaches before considering the special structure of the transition matrix presented by Zucchini, MacDonald, and Langrock (2017), which allows the state dwell distribution to be generalized with arbitrary accuracy. HMMs, or Markov switching processes, have been shown to be appealing models in addressing learning challenges in time series data and have been successfully applied in fields such as speech recognition (Jelinek, 1997; Rabiner, 1989), digit recognition (Rabiner, Wilpon, & Soong, 1989; Raviv, 1967) as well as biological and physiological data (Hadj-Amar, Finkenstädt, Fiecas, & Huckstepp, 2020; Huang et al., 2018; Langrock, Swihart, Caffo, Punjabi, & Crainiceanu, 2013). An HMM is a stochastic process model based on a unobserved (hidden) state sequence $\mathbf{s} = (s_1, \dots, s_T)$ that takes discrete values in the set $\{1, \dots, K\}$ and whose transition probabilities follow a Markovian structure. Conditioned on this state sequence, the observations $\mathbf{y} = (y_1, \dots, y_T)$ are assumed to be conditionally independent and generated from a parametric family of probability distributions $f(\boldsymbol{\theta}_j)$, which are often called *emission* distributions. This generative process can be outlined as

$$\begin{aligned} s_t | s_{t-1} &\sim \boldsymbol{\gamma}_{s_{t-1}} \\ y_t | s_t &\sim f(\boldsymbol{\theta}_{s_t}) \quad t = 1, \dots, T, \end{aligned} \tag{1}$$

where $\boldsymbol{\gamma}_j = (\gamma_{j1}, \dots, \gamma_{jK})$ denotes the state-specific vector of transition probabilities, $\gamma_{jk} = p(s_t = k | s_{t-1} = j)$ with $\sum_k \gamma_{jk} = 1$, and $p(\cdot)$ is a generic notation for probability density or mass function, whichever appropriate. The initial state s_0 has distribution $\boldsymbol{\gamma}_0 = (\gamma_{01}, \dots, \gamma_{0K})$ and $\boldsymbol{\theta}_j$ represents the

vector of emission parameter modelling state j . HMMs provide a simple and flexible mathematical framework that can be naturally used for many inference tasks, such as signal extraction, smoothing, back-tracking and forecasting (see e.g. [Zucchini et al. 2017](#)). These appealing features are a result of an extensive theoretical and methodological literature that includes several dynamic programming algorithms for computing the likelihood in a rather straightforward and inexpensive manner (e.g. forward messages scheme, [Rabiner 1989](#)). HMMs are also naturally suited for local and global decoding (e.g. Viterbi algorithm, [Forney 1973](#)), and the incorporation of trend, seasonality and covariate information in both the observed process and the latent sequence. Although computationally convenient, the Markovian structure of HMMs limits their flexibility. In particular, the *dwell* duration in any state, namely the number of consecutive time points that the Markov chain spends in that state, is implicitly forced to follow a geometric distribution with probability mass function $p(d_j) = (1 - \gamma_{jj}) \gamma_{jj}^{d_j - 1}$.

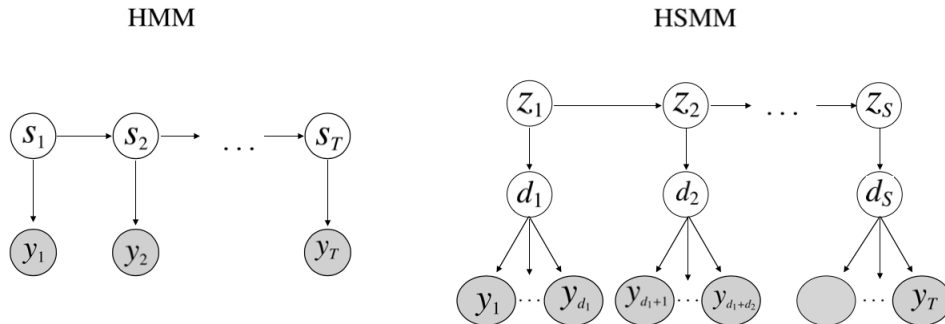


Figure 2: Graphical models: (left) HMM where y_1, \dots, y_T are the observations and s_1, \dots, s_T the corresponding hidden state sequence; (right) HSMM where d_1, \dots, d_S are the random dwell-times associated with each *super* state of the Markov chain z_1, \dots, z_S where no self-transitions are allowed.

A more flexible framework can be formulated using HSMMs, where the generative process of an HMM is augmented by introducing an explicit, state specific, form for the dwell time ([Guédon, 2003](#); [Johnson & Willsky, 2013](#)). The state stays unchanged until the duration terminates, at which point there is a Markov transition to a new regime. As depicted in Figure 2, the *super-states* $\mathbf{z} = (z_1, \dots, z_S)$ are generated from a Markov chain prohibiting self-transitions wherein each super-state z_s is associated with a dwell time d_s and a random segment of observations $\mathbf{y}_s = (y_{t_s^1}, \dots, y_{t_s^2})$, where $t_s^1 = \sum_{r < s} d_r$ and $t_s^2 = t_s^1 + d_s - 1$ represent the first and last index of segment s , and S is the (random) number of segments. Here, d_s represents the length of the dwell duration of z_s . The generative mechanism of an

HSMM can be summarized as

$$\begin{aligned}
z_s | z_{s-1} &\sim \boldsymbol{\pi}_{z_{s-1}} \\
d_s | z_s &\sim g(\boldsymbol{\lambda}_{z_s}) \\
\mathbf{y}_s | z_s &\sim f(\boldsymbol{\theta}_{z_s}) \quad s = 1, \dots, S,
\end{aligned} \tag{2}$$

where $\boldsymbol{\pi}_j = (\pi_{j1}, \dots, \pi_{jK})$ are state-specific transition probabilities in which $\pi_{jk} = p(z_t = k | z_{t-1} = j, z_t \neq k)$ for $j, k = 1, \dots, K$. Note that $\pi_{jj} = 0$, since self transitions are prohibited. We assume that the initial state has distribution $\boldsymbol{\pi}_0 = (\pi_{01}, \dots, \pi_{0K})$, namely $z_0 \sim \boldsymbol{\pi}_0$. Here, g denotes a family of dwell distributions parameterized by some state-specific duration parameters $\boldsymbol{\lambda}_j$, which could be either a scalar (e.g. rate of a Poisson distribution), or a vector (e.g. rate and dispersion parameters for negative-binomial durations). Unfortunately, this increased flexibility in modeling the state duration has the cost of substantially increasing the computational burden of computing the likelihood: the message-passing procedure for HSMMs requires $\mathcal{O}(T^2K + TK^2)$ basic computations for a time series of length T and number of states K , whereas the corresponding forward-backward algorithm for HMMs requires only $\mathcal{O}(TK^2)$.

2.2 Bayesian Approximations to Hidden Semi-Markov Models

Following [Langrock and Zucchini \(2011\)](#), let us consider an HMM in which $\mathbf{y}^* = (y_1^*, \dots, y_T^*)$ represents the observed process and $\mathbf{z}^* = (z_1^*, \dots, z_T^*)$ denotes the latent discrete-valued sequence of a Markov chain with states $\{1, 2, \dots, \bar{A}\}$, where $\bar{A} = \sum_{j=1}^K a_j$, and a_1, \dots, a_K are arbitrarily fixed positive integers. Let us define *state aggregates* A_j as

$$A_j = \left\{ a : \sum_{i=0}^{j-1} a_i < a \leq \sum_{i=0}^j a_i \right\}, \quad j = 1, \dots, K, \tag{3}$$

where $a_0 = 0$, and each state corresponding to A_j is associated with the same emission distribution $f(\boldsymbol{\theta}_j)$ in the HSMM formulation of Equation (2), namely $y_t^* | z_t^* \in A_j \sim f(\boldsymbol{\theta}_j)$. The probabilistic rules governing the transitions between states \mathbf{z}^* are described via the matrix $\boldsymbol{\Phi} = \{\phi_{il}\}$, where $\phi_{il} = p(z_t^* = l | z_{t-1}^* = i)$, for $i, l = 1, \dots, \bar{A}$. This matrix has the following structure

$$\boldsymbol{\Phi} = \begin{bmatrix} \boldsymbol{\Phi}_{11} & \dots & \boldsymbol{\Phi}_{1K} \\ \vdots & \ddots & \vdots \\ \boldsymbol{\Phi}_{K1} & \dots & \boldsymbol{\Phi}_{KK} \end{bmatrix}, \tag{4}$$

where the diagonal matrices Φ_{jj} of dimension $a_j \times a_j$, are defined, for $a_j \geq 2$, as

$$\Phi_{jj} = \begin{bmatrix} 0 & 1 - h_j(1) & 0 & \dots & 0 \\ \vdots & 0 & \ddots & & \vdots \\ & \vdots & & & 0 \\ 0 & 0 & \dots & 0 & 1 - h_j(a_j - 1) \\ 0 & 0 & \dots & 0 & 1 - h_j(a_j) \end{bmatrix}, \quad (5)$$

and $\Phi_{jj} = 1 - h_j(1)$, for $a_j = 1$. The $a_j \times a_k$ off-diagonal matrices Φ_{jk} are given by

$$\Phi_{jk} = \begin{bmatrix} \pi_{jk} h_j(1) & 0 & \dots & 0 \\ \pi_{jk} h_j(2) & 0 & \dots & 0 \\ \vdots & & & \\ \pi_{jk} h_j(a_j) & 0 & \dots & 0 \end{bmatrix} \quad (6)$$

where in the case that $a_j = 1$ only the first column is included. Here, π_{jk} are the transition probabilities of an HSMM as in Equation (2), and the *hazard rates* $h_j(r)$ are specified for $r \in \mathbb{N}_{>0}$ as

$$h_j(r) = \frac{p(d_j = r | \boldsymbol{\lambda}_j)}{p(d_j \geq r | \boldsymbol{\lambda}_j)}, \quad \text{if } p(d_j \geq r - 1 | \boldsymbol{\lambda}_j) < 1, \quad (7)$$

and 1 otherwise, where $p(d_j = r | \boldsymbol{\lambda}_j)$ denotes the probability mass function of the dwell distribution $g(\boldsymbol{\lambda}_j)$ for state j . This structure for the matrix Φ implies that transitions within state aggregate A_j are determined by diagonal matrices Φ_{jj} , while transitions between state aggregates A_j and A_k are controlled by off-diagonal matrices Φ_{jk} . Additionally, a transition from A_j to A_k must enter A_k in $\min(A_k)$. [Langrock and Zucchini \(2011\)](#) showed that this choice of Φ allows to represent any duration distribution, and yields an HMM that is, at least approximately, a reformulation of a given HSMM. In summary, the distribution of \mathbf{y} can be approximated by that of \mathbf{y}^* , and this approximation can be designed to be arbitrarily accurate by choosing the a_j adequately large. In fact, the accuracy in representing the dwell distribution through Φ differs from the true distribution, namely the one in the HSMM formulation of Equation (2), only for values larger than a_j , i.e., in the right tail.

The generative process of our Bayesian model can be summarized by

$$\begin{aligned} \boldsymbol{\pi}_j &\sim \text{Dir}(\boldsymbol{\alpha}_0), & (\boldsymbol{\theta}_j, \boldsymbol{\lambda}_j) &\sim H \times G, & j &= 1, \dots, K, \\ z_t^* | z_{t-1}^* &\sim \phi_{z_{t-1}^*} & & & & (8) \\ \mathbf{y}_t^* | z_t^* \in A_j &\sim f(\boldsymbol{\theta}_j) & & & t &= 1, \dots, T, \end{aligned}$$

where $\text{Dir}(\cdot)$ denotes the Dirichlet distribution over a $(K-2)$ dimensional simplex (since the probability of self transition is forced to be zero) and $\boldsymbol{\alpha}_0$ is a vector of positive reals. Here, H and G represent the priors over emission and duration parameters, respectively, and ϕ_i denotes the i^{th} row of the matrix Φ . A graphical model representing the probabilistic structure of our approach is shown in Figure 3, where we remark that the entries of the transition matrix Φ are entirely determined by the transition probabilities of the Markov chain π_j and the values of the durations $p(d_j = r | \lambda_j)$.

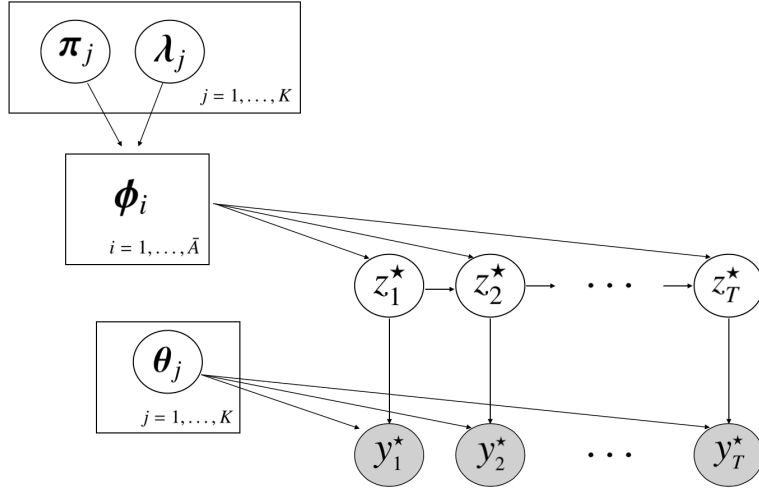


Figure 3: A graphical model for Equation (8). Transition probabilities ϕ_j are solely determined by π_j and $p(d_j = r | \lambda_j)$, and thus they are not considered as random variable themselves.

3 Inference

Our inference scheme for estimating the parameters $\boldsymbol{\eta} = \{(\pi_j, \lambda_j, \theta_j)\}_{j=1}^K$ is formulated within a full Bayesian framework and it is based on the following factorization of the joint posterior distribution

$$p(\boldsymbol{\eta} | \mathbf{y}) \propto \mathcal{L}(\mathbf{y} | \boldsymbol{\eta}) \times \left[\prod_{j=1}^K p(\pi_j) \times p(\lambda_j) \times p(\theta_j) \right], \quad (9)$$

where $\mathcal{L}(\cdot)$ denotes the likelihood of the model, $p(\pi_j)$ is the density of the Dirichlet prior for transitions probabilities (Equation 2.2), and $p(\lambda_j)$ and $p(\theta_j)$ represent the prior densities for dwell and emission parameters, respectively. Since we have formulated an HMM, we can employ well-known techniques that are available to compute the likelihood, and in particular we can express it using the

following matrix multiplication (see e.g. [Zucchini et al. 2017](#))

$$\mathcal{L}(\mathbf{y}|\boldsymbol{\eta}) = \boldsymbol{\pi}_0^{\star'} \mathbf{P}(y_1) \boldsymbol{\Phi} \mathbf{P}(y_2) \boldsymbol{\Phi} \cdots \boldsymbol{\Phi} \mathbf{P}(y_{T-1}) \boldsymbol{\Phi} \mathbf{P}(y_T) \mathbf{1}, \quad (10)$$

where the diagonal matrix $\mathbf{P}(y)$ of dimension $\bar{A} \times \bar{A}$ is defined as

$$\mathbf{P}(y) = \text{diag} \left\{ \underbrace{p(y|\boldsymbol{\theta}_1), \dots, p(y|\boldsymbol{\theta}_1)}_{a_1 \text{ times}}, \dots, \underbrace{p(y|\boldsymbol{\theta}_K) \dots p(y|\boldsymbol{\theta}_K)}_{a_K \text{ times}} \right\}, \quad (11)$$

and $p(y|\boldsymbol{\theta}_j)$ is the probability density of the emission distribution $f(\boldsymbol{\theta}_j)$. Here, $\mathbf{1}$ denotes an \bar{A} -dimensional column vector with all entries equal to one and $\boldsymbol{\pi}_0^{\star}$ represents the initial distribution for the state aggregates. Note that if we assume that the underlying Markov chain is stationary, $\boldsymbol{\pi}_0^{\star}$ is solely determined by the transition probabilities $\boldsymbol{\Phi}$, i.e. $\boldsymbol{\pi}_0^{\star} = (\mathbf{I} - \boldsymbol{\Phi} + \mathbf{U})^{-1} \mathbf{1}$, where \mathbf{I} is the identity matrix and \mathbf{U} being a square matrix of ones. Alternatively, it is possible to start from a specified state, namely assuming that $\boldsymbol{\pi}_0^{\star}$ is an appropriate unit vector, e.g. $(1, 0, \dots, 0)$, as suggested by [Leroux and Puterman \(1992\)](#). We finally note that computation of the likelihood (10) is often subject to numerical underflow and hence its practical implementation usually require appropriate scaling ([Zucchini et al., 2017](#)).

While a full Bayesian framework is desirable for its ability to provide coherent uncertainty quantification for parameter values, a perceived draw back of this approach compared with a frequentist analogue is the increased computation required for the estimation. Bayesian posterior distributions are only available in closed form under the very restrictive setting when the likelihood and prior are conjugate. Unfortunately, the model outlined in [Section 2.2](#) does not emit such a conjugate prior form and as a result the corresponding posterior ([Equation 9](#)) is not analytically tractable. However, numerical methods such as Markov Chain Monte Carlo (MCMC) can be employed to sample from this intractable posterior. The last twenty years has seen an explosion of research into MCMC methods and more recently approaches scaling them to high dimensional parameter spaces. The next section outlines one such black box implementation that is used to sample from the posterior in [Equation \(9\)](#).

3.1 Hamiltonian Monte Carlo, No-U-Turn Sampler and Stan Modelling Language

One particularly successful posterior sampling algorithm is Hamiltonian Monte Carlo (HMC, [Duane, Kennedy, Pendleton, and Roweth 1987](#)), where we refer the reader to [Neal et al. \(2011\)](#) for an excellent introduction. HMC augments the parameter space with a ‘momentum variable’ and uses Hamiltonian

dynamics to propose new samples. The gradient information contained within the Hamiltonian dynamics allows HMC to produce proposals that can traverse high dimensional spaces more efficiently than standard random walk MCMC algorithms. However, the performance of HMC samplers is dependent on the tuning of the leapfrog discretisation of the Hamiltonian dynamics. The No-U-Turn Sampler (NUTS) (Hoffman & Gelman, 2014) circumvents this burden. NUTS uses the Hamiltonian dynamics to construct trajectories that move away from the current value of the sampler until they make a ‘U-Turn’ and start coming back, thus maximising the trajectory distance. An iterative algorithm allows the trajectories to be constructed both forwards and backwards in time, preserving time reversibility. Combined with a stochastic optimisation of the step size, NUTS is able to conduct efficient sampling without any hand tuning.

The *stan* modelling language (Carpenter et al., 2016) provides a probabilistic programming environment facilitating the easy implementation of NUTS. The user need only define the three component of their model: (i) the inputs to their sampler, e.g. data and prior hyperparameters; (ii) the outputs, e.g. parameters of interest; (iii) the computation required to calculate the unnormalized posterior. Following this, *stan* uses automatic differentiation (Griewank & Walther, 2008) to produce fast and accurate samples from the target posterior. *stan*’s easy to use interface and lack of required tuning has seen it implemented in many areas of statistical science. As well as using NUTS to automatically tune the sampler, *stan* is equipped with a variety of warnings and tools to help users diagnose the performance of their sampler. For example, convergence of all quantities of interest is monitored in automated fashion by comparing variation between and within simulated samples initialized at over-dispersed starting values (Gelman, Simpson, & Betancourt, 2017). Additionally, the structure of the transition matrix Φ allows us to take advantage of *stan*’s sparse matrix implementation to achieve vast computational improvements. Although Φ has dimension $\bar{A} \times \bar{A}$, each row has at most K non-zero terms (representing within state transitions to the next state aggregate or between state transitions), and as a result Φ has (K/\bar{A}) non zero elements. Hence, for large values of the dwell approximation thresholds \mathbf{a} , the matrix Φ exhibits considerable sparsity. The *stan* modelling language implements compressed row storage sparse matrix representation and multiplication, which provides considerable speed up when the sparsity is greater than 90% (Stan Development Team, 2018, Ch. 6). In our applied scenario we consider dwell-approximation thresholds as big as $\mathbf{a} = (150, 10, 10)$ with sparsity of greater than 98% allowing us to take considerable advantage of this formulation. Finally, we note that our proposed Bayesian approach may suffer from *label switching* (Stephens, 2000) since

the likelihood is invariant under permutations of labelling of the hidden states. However, this issue is easily addressed using order constraints provided by *stan*.

3.2 Bridge Sampling Estimation of the Marginal Likelihood

The Bayesian paradigm provides a natural framework for selecting between competing models by means of the marginal likelihood, i.e.

$$p(\mathbf{y}) = \int \mathcal{L}(\mathbf{y} | \boldsymbol{\eta}) p(\boldsymbol{\eta}) d\boldsymbol{\eta}. \quad (12)$$

The ratio of marginal likelihoods from two different models, often called the *Bayes factor* (Kass & Raftery, 1995), can be thought of as the weight of evidence in favor of a model against a competing one. The marginal likelihood (12) corresponds to the normalizer of the posterior $p(\boldsymbol{\eta} | \mathbf{y})$ (Eq. 9) and is generally the component that makes the posterior analytically intractable. MCMC algorithms, such as the *stan*’s implementation of NUTS introduced above, allow for sampling from the unnormalized posterior, but further work is required to estimate the normalizing constant. Bridge sampling (Meng & Schilling, 2002; Meng & Wong, 1996) provides a general procedure for estimating these marginal likelihoods reliably. While standard Monte Carlo (MC) estimates draw samples from a single distribution, bridge sampling formulates an estimate of the marginal likelihood using the ratio of two MC estimates drawn from different distributions: one being the posterior (which has already been sampled from) and the other being an appropriately chosen proposal distribution $q(\boldsymbol{\eta})$. The bridge sampling estimate of the marginal likelihood is then given by

$$p(\mathbf{y}) = \frac{\mathbb{E}_{q(\boldsymbol{\eta})} [h(\boldsymbol{\eta}) \mathcal{L}(\mathbf{y} | \boldsymbol{\eta}) p(\boldsymbol{\eta})]}{\mathbb{E}_{p(\boldsymbol{\eta} | \mathbf{y})} [h(\boldsymbol{\theta}) q(\boldsymbol{\theta})]} \approx \frac{\frac{1}{n_2} \sum_{j=1}^{n_2} h(\tilde{\boldsymbol{\eta}}^{(j)}) \mathcal{L}(\mathbf{y} | \tilde{\boldsymbol{\eta}}^{(j)}) p(\tilde{\boldsymbol{\eta}}^{(j)})}{\frac{1}{n_1} \sum_{i=1}^{n_1} h(\bar{\boldsymbol{\eta}}^{(i)}) q(\bar{\boldsymbol{\eta}}^{(i)})},$$

where $h(\boldsymbol{\eta})$ is an appropriately selected *bridge function* and $p(\boldsymbol{\eta})$ denotes the joint prior distribution. Here, $\{\bar{\boldsymbol{\eta}}^{(1)}, \dots, \bar{\boldsymbol{\eta}}^{(n_1)}\}$ and $\{\tilde{\boldsymbol{\eta}}^{(1)}, \dots, \tilde{\boldsymbol{\eta}}^{(n_2)}\}$ represent n_1 and n_2 samples drawn from the posterior $p(\boldsymbol{\eta} | \mathbf{y})$ and the proposal distribution $q(\boldsymbol{\eta})$, respectively. This estimator can be implemented in R using the package `bridgesampling` (Gronau et al., 2020), whose compatibility with *stan* makes it particularly straightforward to estimate the marginal likelihood directly from a *stan* output. This package implements the method of Meng and Wong (1996) to choose the optimal bridge function minimising the estimator mean-squared error and constructs a multivariate normal proposal distribution whose mean and variance match those of the sample from the posterior.

3.3 Comparable Dwell Priors

Model selection based on marginal likelihoods can be very sensitive to prior specifications. In fact, Bayes factors are only defined when the marginal likelihood under each competing model is proper (Gelman et al., 2013; Robert, 2007). As a result, it is important to include any available prior information into the Bayesian modelling in order to use these quantities in a credible manner. Reliably characterising the prior for the dwell distributions is particularly important for the experiments considered in Section 5, since we use Bayesian marginal likelihoods to select between the dwell distributions associated with HSMMs and HMMs. For instance, if we believe that the length of sleep for an average person is between 7 and 8 hours we would choose a prior that reflects those beliefs in all competing models. However, we need to ensure that we encode this information in *comparable priors* in order to perform ‘fair’ Bayes factor selection amongst a set of dwell-distributions. Our aim is to infer which dwell distribution, and not which prior specification, is most appropriate for the data at hand.

For example, suppose we consider selecting between geometric (i.e. an HMM), negative-binomial or Poisson distributions (i.e. an HSMM), to model the dwell durations of our data. While a Poisson random variable, shifted away from zero to consider strictly positive dwells, has its mean $\lambda_j + 1$ and variance λ_j described by the same parameter λ_j , the negative-binomial allows for further modelling of the precision through an additional factor ρ_j . In both negative-binomial and Poisson HSMMs, the parameters λ_j are usually assigned a prior $\lambda_j \sim \text{Gamma}(a_{0j}, b_{0j})$ with mean $\mathbb{E}[\lambda_j] = a_{0j}/b_{0j}$ and variance $\text{Var}[\lambda_j] = a_{0j}/b_{0j}^2$. In order to develop an interpretable comparison of all competing models, we parameterize the geometric dwell distribution associated with state j in the standard HMM (Eq. 1) as also being characterized by the mean dwell length $\tau_j = 1/(1 - \gamma_{jj})$, where the geometric is also shifted to only consider strictly positive support and γ_{jj} represents the probability of self-transition. Under a Dirichlet prior for the state-specific vector of transition probabilities $\boldsymbol{\gamma}_j = (\gamma_{j1}, \dots, \gamma_{jK}) \sim \text{Dirichlet}(\mathbf{v}_j)$, with $\mathbf{v}_j = (v_{j1}, \dots, v_{jK})$ and $\beta_j = \sum_{i \neq j} v_{ji}$, the mean and variance of the prior mean dwell under an HMM are given by

$$\mathbb{E}[\tau_j] = \frac{v_{jj} + \beta_j - 1}{\beta_j - 1} \text{ and } \text{Var}[\tau_j] = \frac{(v_{jj} + \beta_j - 1)(v_{jj} + \beta_j - 2)}{(\beta_j - 1)(\beta_j - 2)} - \left(\frac{v_{jj} + \beta_j - 1}{\beta_j - 1} \right)^2$$

for $\beta_j > 2$ (the derivation of this result is provided in the Supplementary Material).

We therefore argue that a comparable prior specification requires hyper-parameters $\{a_{0j}, b_{0j}\}_{j=1}^K$ and $\{\mathbf{v}_j\}_{j=1}^K$ be chosen in a way that satisfy $\mathbb{E}[\tau_j] = \mathbb{E}[\lambda_j + 1]$ and $\text{Var}[\tau_j] = \text{Var}[\lambda_j + 1]$, ensuring the mean dwell distribution in each state has the same prior mean and variance across models. The

prior mean can be interpreted as a best a priori guess for the average dwell time in each state, and the variance reflects the confidence in this prior belief. In addition, since the negative-binomial distribution is further parameterized by a dispersion parameter ρ_j , we center our prior belief at $\rho_j = 1$, which is the value that recovers geometric dwell durations (namely an HMM) when $\lambda_j = \gamma_{jj}/(1 - \gamma_{jj})$. Between state transition probabilities, i.e. the non-diagonal entries of the transition matrix, as well as the emission parameters, are shared between the HMM and HSMM, and thus we may place a prior specification on these parameters that is common across all models.

4 Simulation Studies

We conduct simulation studies to illustrate the performance of our proposed procedure and demonstrate the benefits of using a Bayesian approach. We choose not to discuss the philosophical desirability of either the frequentist or Bayesian paradigm here, since this has been considered at length before (e.g. Cox 2006; Robert 2007). Instead we focus on the practical implications of the difference in these two approaches and in particular we explain some of the potential drawbacks of using frequentist methodologies for parameter inference, prediction and model selection. Supplementary Material (see also <https://github.com/Beniamino92/BayesianApproxHSMM>) contains the *stan* files, as well as R utilities, that were used to implement the Bayesian analysis for our experiments. The probabilistic programming framework associated with *stan* makes it easy for practitioners to consider further dwell/emission distributions to the ones considered here. Users need only to change the corresponding function in our *stan* files.

4.1 Prior Regularization, Dwell Threshold and Forecasting

In this example, we simulated a time series consisting of $T = 200$ data points from a three-state HSMM (Equation 2). Conditional on each state j , the observations are generated from a Normal (μ_j, σ_j^2) , and the dwell durations are Poisson(λ_j) distributed. We consider relatively large values for λ_j in order to evaluate the quality of the HSMM approximation provided by Equation (8). The full parameterization is provided in Table 1 and a realization of this model is shown in Figure 4 (a, top). The dwell thresholds \mathbf{a} are set equal to (30, 30, 30) and we placed a Gamma(0.01, 0.01) prior on the Poisson rates λ_j . The transition probabilities $\boldsymbol{\pi}_j$ are distributed as Dirichlet(1, 1) and the priors for the Gaussian emissions are given as Normal(0, 10^2) and Inverse-Gamma(2, 0.5) for locations μ_j and scale σ_j^2 , respectively.

Note that, overall, this prior specification reflects some rather weakly informative beliefs (Gelman et al., 2013, 2017). Our proposed methodology is run for 6,000 iterations, 1,000 of which are discarded as burn-in, where the full estimation algorithm took 2086 seconds on an Intel® Core™ i7 2.2 GHz Processor 8 GB RAM.

	True	EM	Bayes		True	EM	Bayes		True	EM	Bayes
μ_1	5	4.96	4.95 (4.66 - 5.24)	σ_3	1	1.01	1.08 (0.90 - 1.20)	π_{13}	0.70	0.50	0.5 (0.13 - 0.87)
μ_2	14	14.02	14.02 (13.67 - 14.37)	λ_1	20	23.47	23.36 (17.03 - 30.57)	π_{21}	0.20	0.00	0.20 (0.01 - 0.53)
μ_3	30	30.19	30.18 (29.98 - 30.38)	λ_2	30	27.22	27.05 (22.43 - 32.19)	π_{23}	0.80	1.00	0.80 (0.47 - 0.99)
σ_1	1	1.09	1.15 (0.95 - 1.40)	λ_3	20	19.98	20.00 (15.93 - 24.46)	π_{31}	0.10	0.33	0.40 (0.10 - 0.76)
σ_2	2	1.90	1.95 (1.73 - 2.22)	π_{12}	0.30	0.50	0.50 (0.13 - 0.87)	π_{32}	0.90	0.67	0.60 (0.24 - 0.90)

Table 1: Illustrative Example. True model parameterization and corresponding estimates obtained via the EM algorithm and our proposed Bayesian approach. For the latter, we also report 95% credible intervals obtained from the posterior sample.

Table 1 shows estimation results for our proposed Bayesian methodology as well as the analogue frequentist approach (EM) as in Langrock and Zucchini (2011). While it is clear that both methods satisfactorily retrieve the correct pre-fixed duration and emission parameters, our proposed methodology further provides a measure of uncertainty which is given by the 95% credible intervals obtained from the posterior sample. Although we acknowledge that frequentists can produce confidence measures such as standard errors and bootstrap estimates, we note that those quantities are not automatically provided by the EM and cannot be naturally adapted for prediction or model selection. As depicted in Figure 4 (b), an additional advantage of our Bayesian paradigm is reflected in the estimation of the transition probabilities. For example, note that the true generating value for π_{21} is set to 0.2 but this time-series realization (Figure 4 a, top) shows no transitions from state 2 to state 1. The EM algorithm incorrectly estimates π_{12} as zero, while our methodology considers full uncertainty quantification and

uses a flat prior on the transitions, yielding a significantly more reliable estimate. Figure 4 (a) also displays: (top) a graphical posterior predictive check consisting of the observations alongside 100 draws from the estimated posterior predictive (Gelman et al., 2013), the latter obtained by first drawing a sample path using a variant of the forward-backward procedure (see e.g. Hadj-Amar et al. 2020), and then, conditioned on the hidden state sequence, the predicted values are simulated from appropriate emission distributions. It is clear that no systematic discrepancies between observed and predicted data can be noticed; (bottom) the most likely hidden state sequence, i.e. $\arg \max_{\mathbf{z}} p(\mathbf{z} | \mathbf{y}, \boldsymbol{\eta})$, which is estimated via the Viterbi algorithm (see e.g. Zucchini et al. 2017) using plug-in Bayes estimates of the model parameters; In order to assess the goodness of fit of the model, we also verified normality of the pseudo-residual (see Supplementary Material).

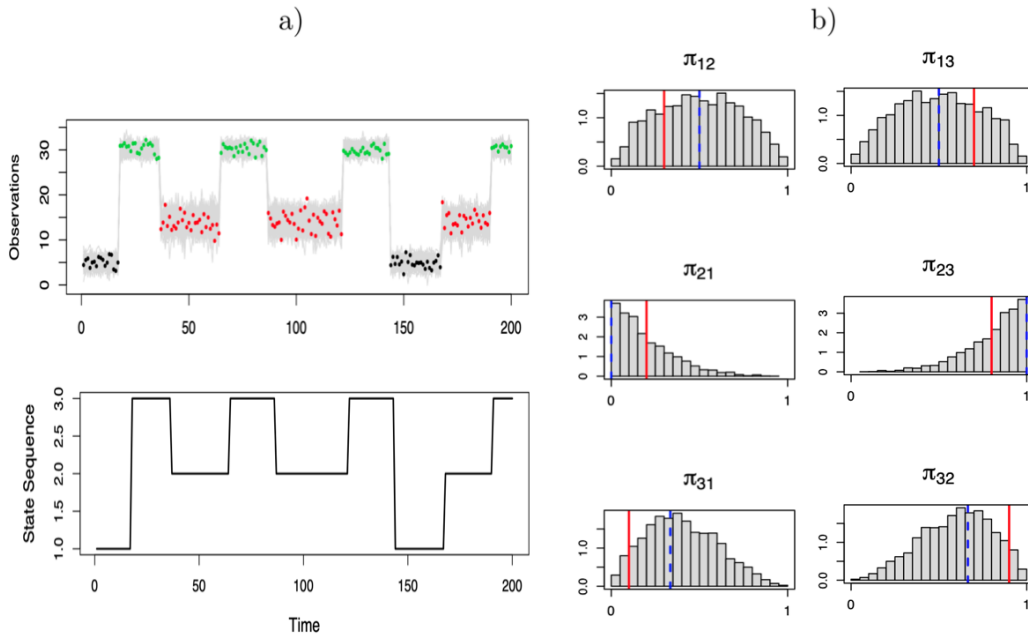


Figure 4: (a, top) a realization (dots) of a three-state HSM with Gaussian emissions and Poisson durations, where different colors correspond to (true) different latent state. Grey lines represent 100 samples drawn from the estimated posterior predictive distribution, showing that our predictions line up correctly with the true values. (a, bottom) most likely hidden state sequence estimated via the Viterbi algorithm; (b) estimated posterior distribution of the transition probabilities π_{jk} , where vertical solid red and blue dotted lines represent true values and EM estimates, respectively. Our proposed methodology considers full uncertainty quantification, yielding more reliable estimates.

The impact of approximating the dwell distribution is investigated in Table 2, where we computed likelihood and marginal likelihood for different choices of the dwell threshold \mathbf{a} . These performance measures were also estimated using an HSMM (i.e. the true data generating process) and a Bayesian HMM. The HSMM estimation was carried out in a frequentist fashion using the R package `hsmm` (Bulla, Bulla, & Nenadić, 2010). Note that in this illustrative example we consider λ_j , the mean of the dwell distributions, to be of similar size or greater than the approximation thresholds \mathbf{a} . Under the approximation to the HSMM used here, the dwell distribution matches that of the exact HSMM up until the approximation threshold, while after this point the dwell distribution behaves geometrically. Having the approximation cutoff above the average dwell time results in a significant amount of the dwell mass being approximated. Note that though larger values of \mathbf{a} allow for better approximations to the specified dwell-time distribution, these come at a computational cost of increasing the size of the transition probability matrix Φ . This cost can be somewhat mitigated by the sparse nature of the transition matrix, as discussed in Section 3.1. However as with any large scale analysis, a trade-off between statistical accuracy and computationally feasibility must be reached. While it is evident that more accurate approximations are achieved for larger \mathbf{a} , it also appears that choosing values smaller than $\mathbf{a} = (30, 30, 30)$ can still yield satisfactory inference. In fact, in all simulation settings we are retrieving the correct emission parameters and performance measures are not far from an HSMM. In addition, the likelihood statistics show that these approximations improve upon the HMM significantly.

Table 2: Performance measures for HSMM, HMM, and our proposed approach for different values of \mathbf{a} . The negative of the log-likelihood (evaluated pointwise) and marginal log-likelihood (only for Bayesian methods) are reported, as well as the estimate of the rate λ_j of the distinct dwell-distributions.

	- llk	marg llk	λ_1	λ_2	λ_3
HSMM	368.49	-	19.50	27.67	20.21
HMM	382.15	-425.93	-	-	-
Proposed: $\mathbf{a} = (5, 5, 5)$	377.92	-425.65	8.25	8.85	8.38
Proposed: $\mathbf{a} = (10, 10, 10)$	375.16	-423.36	14.24	13.28	13.14
Proposed: $\mathbf{a} = (20, 20, 20)$	368.79	-417.06	20.74	22.87	19.51
Proposed: $\mathbf{a} = (30, 30, 30)$	366.43	-414.50	23.36	27.05	20.00

We evaluate the forecasting properties of both frequentist and Bayesian approaches on a test set $\tilde{\mathbf{y}} = (\tilde{y}_1, \dots, \tilde{y}_H)$, where $\tilde{y}_h = y_{T+h}$, $h = 1, \dots, H$, and $H \in \mathbb{N}_{>0}$ denotes the forecast horizon. Here, we used the logarithmic score (log-score) to measure predictive performances, while acknowledging that other scoring rules may be equally valid. Let $\hat{\boldsymbol{\eta}}$ be the frequentist (MLE/EM) parameter estimate and define the log-score

$$L_{\text{freq}}(\tilde{\mathbf{y}}) = \sum_{h=1}^H \log p(\tilde{y}_h | \hat{\boldsymbol{\eta}}),$$

where $p(\tilde{y}_h | \hat{\boldsymbol{\eta}})$ denotes the forecast density function (see Supplementary Material for an explicit expression). Our Bayesian framework does not assume a point estimate $\hat{\boldsymbol{\eta}}$ but considers instead a posterior distribution $p(\boldsymbol{\eta} | \mathbf{y})$. Rather than making predictions using a plugin estimate, we hence integrate out the model parameters and evaluate the predictive density of a future observation \tilde{y}_h . This is achieved by approximating the following predictive distribution

$$p(\tilde{y}_h | \mathbf{y}) = \int p(\tilde{y}_h | \boldsymbol{\eta}) p(\boldsymbol{\eta} | \mathbf{y}) d\boldsymbol{\eta} \approx \frac{1}{M} \sum_{i=1}^M p(\tilde{y}_h | \boldsymbol{\eta}^{(i)}),$$

where $\boldsymbol{\eta}^{(i)}$ represent a draw from $p(\boldsymbol{\eta} | \mathbf{y})$ and M is total number of MCMC iterations. As a result, the Bayesian predictive log-score becomes

$$L_{\text{Bayes}}(\tilde{\mathbf{y}}) = \sum_{h=1}^H \log \left(\frac{1}{M} \sum_{i=1}^M p(\tilde{y}_h | \boldsymbol{\eta}^{(i)}) p(\boldsymbol{\eta}^{(i)} | \mathbf{y}) \right), \quad \{\boldsymbol{\eta}^{(i)}\}_{i=1}^M \sim \pi(\boldsymbol{\eta} | \mathbf{y}).$$

We simulated 20 time series from the same model as in Table 1, for different forecast horizons $H = 100, 300, 500$. Figure 5 presents box-plots of log-scores for the EM algorithm and our proposed Bayesian approach. It is clear that a Bayesian methodology, which considers full uncertainty quantification, typically produces a much lower predictive log-score than a frequentist procedure. The latter approach, which uses plug-in estimates for parameters, is known to ‘under-estimate’ the true predictive variance thus yielding large values of the log-score (Jewson, Smith, & Holmes, 2018). On the other hand, our Bayesian paradigm integrates over the parameters and hence is more accurately able to capture the true forecast distribution. As a result, it produces significantly smaller log-score estimates. In fact, (Aitchison, 1975) showed that, under repeat sampling, the Bayesian predictive is closer, in terms of Kullback-Leibler divergence, to the true underlying distribution than its frequentist plug-in counterpart.

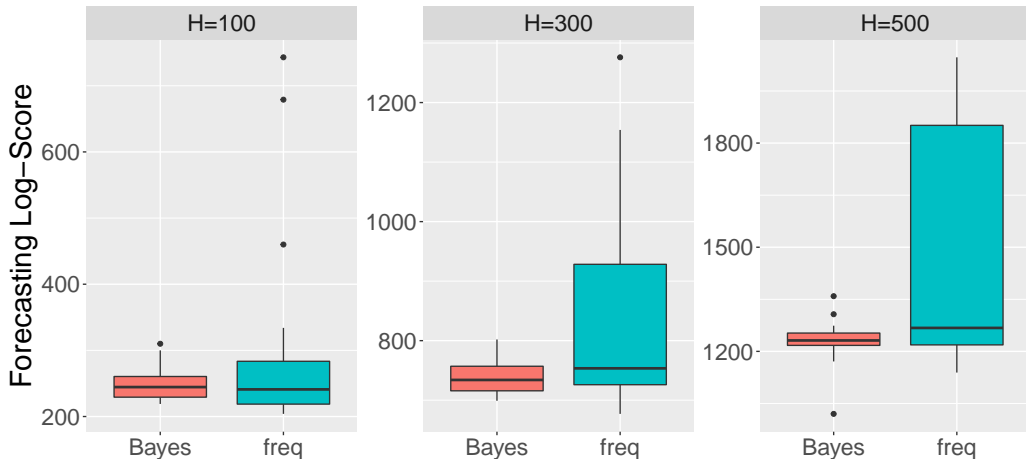


Figure 5: Boxplots of log-scores for both EM and our Bayesian methodology, with three different forecast horizons $H = 100, 300, 500$. It is evident that a Bayesian approach is superior in terms of forecasting performance.

4.2 AIC, BIC and Marginal Likelihood

When analyzing time series, we may wonder whether to formulate an HMM or to extend the dwell distribution beyond a geometric one (i.e., an HSMM). Ideally, the data should be used to drive such a decision. In this section we compare the frequentist methods for doing so, namely Akaike’s information criterion (AIC, [Akaike 1973](#)) and Bayesian information criterion (BIC, [Schwarz et al. 1978](#)), with their Bayesian counterpart, namely the marginal likelihood. We show some of the potential drawbacks of using frequentist methodologies when choosing among competing nested models. We choose not to consider other Bayesian inspired information criteria, for example the Deviance information criteria (DIC, [Spiegelhalter, Best, Carlin, and Van Der Linde 2002](#)) or the Watanabe-Akaike information criterion (WAIC, [Watanabe 2010](#)), see [Gelman, Hwang, and Vehtari \(2014\)](#) for an excellent review of these approaches within the Bayesian paradigm. Our goal here is to compare standard frequentist methods used previously in the literature to conduct model selection for HMMs and HSMMs (e.g. [Huang et al., 2018](#); [Langrock & Zucchini, 2011](#)) with the canonical Bayesian analog.

4.2.1 Consistency for Nested Models

Let us consider two models $\mathcal{L}_1(\mathbf{y}|\boldsymbol{\eta}_1)$ for $\boldsymbol{\eta}_1 \in \mathbf{H}_1$ and $\mathcal{L}_2(\mathbf{y}|\boldsymbol{\eta}_2)$ for $\boldsymbol{\eta}_2 \in \mathbf{H}_2$. If $\mathbf{H}_1 \subset \mathbf{H}_2$, we say model \mathcal{L}_1 is *nested* within \mathcal{L}_2 . As a result, there exist values of the parameters $\boldsymbol{\eta}_2$ that allow

the likelihood \mathcal{L}_2 to match \mathcal{L}_1 . An example of this scenario comes in linear regression where a model with fewer covariates is recovered from one with more when the coefficients for the additional covariates are equal to zero. Being more complex, \mathcal{L}_2 always achieves higher values for the maximised log-likelihoods than \mathcal{L}_1 when evaluated on the same data. As a result, simpler models can only be selected if the complexity of the models is somehow penalized. The AIC $:= -2 \mathcal{L}(\mathbf{y} | \boldsymbol{\eta}) + 2p$ is known not to provide consistent model selection amongst nested models when the data is generated from the simplest one (see e.g. [Fujikoshi, 1985](#)), where here p denotes the number of parameters included in the model. This metric penalizes complexity through the term $2p$, which does not depend on the number of data points T . Thus, as T tends to infinity there is still a chance that an increased likelihood can overwhelm the complexity penalty, yielding a non-zero probability that AIC will incorrectly select the more complicated model. On the other hand, performing model selection using the marginal likelihood can be shown to be consistent (see e.g. [O’Hagan and Forster 2004](#)), provided some weak conditions on the prior are satisfied. Therefore, when following a Bayesian paradigm, the correct data generating model is selected with probability one (as T tends to infinity). We illustrate the above concepts by considering two cases of model nesting when selecting between HSMMs and HMMs: (i) the negative-binomial likelihood, parameterized by its mean λ and dispersion parameter ρ , recovers the geometric distribution as a special case when $\rho = 1$; (ii) the unstructured start geometric tail distribution ([Sansom & Thomson, 2001](#)), parameterized by $\boldsymbol{\epsilon} = (\epsilon_1, \dots, \epsilon_m)$, has mass function

$$p(r | \boldsymbol{\epsilon}) = \begin{cases} \epsilon_r & \text{if } r \leq m, \\ \epsilon_m \left(1 - \frac{\epsilon_m}{(1 - \sum_{i=1}^{m-1} \epsilon_i)}\right)^{r-m} & \text{otherwise,} \end{cases}$$

and recovers the geometric distribution when $m = 1$. For $m > 1$, the geometric distribution is nested within the unstructured geometric since the right tail remains geometric and the left tail has the flexibility through $\boldsymbol{\epsilon}$ to capture the geometric pmf.

We simulated 20 time series from a two state HMM with Gaussian emissions parameters $\boldsymbol{\mu} = (1, 4)$ and $\boldsymbol{\sigma}^2 = (1, 1.5)$, and diagonal entries of the transition matrix set to $(\gamma_{11}, \gamma_{22}) = (0.7, 0.6)$. We ran the estimation algorithms for the HMM and HSMM with unstructured start geometric tail durations and $\mathbf{m} = (2, 1)$, using both frequentist and Bayesian methodologies (further experiments involving different unstructured start geometric tail and negative-binomial durations are provided in the Supplementary Material). For the HSMM approximation, we select $\mathbf{a} = \mathbf{m} = (2, 2)$ thus the dwell distribution is exactly modelled. We use prior distributions that are comparable as explained in [Section 3.3](#), the

exact prior specifications are presented in the Supplementary Material. Figure 6 (top) displays box-plots of the difference between the model selection criteria (namely marginal likelihood and AIC) achieved by the HMM and the HSMM, for increasing sample size $T = 500, 5000, 10000$. We negate the AIC such that maximising both criteria is desirable. Thus, positive values for the difference correspond to correctly selecting the simpler data generating model, i.e. the HMM. As the sample size T increases, the marginal likelihood appears to converge to a positive value and the variance across repeats decreases, indicating consistent selection of the correct model. On the other hand, even as T gets larger there are still occasions when the AIC strongly favours the incorrect more complicated model, which is a symptom of the lack of consistency exhibited by AIC.

4.2.2 Complexity Penalization

Unlike the AIC, the BIC $:= -2\mathcal{L}(\mathbf{y}|\boldsymbol{\eta}) + p\log T$ penalizes complexity in a manner that depends on the sample size T . This frequentist model selection criterion is termed ‘Bayesian’ because it corresponds to the Laplace approximation of the marginal likelihood of the data (Konishi & Kitagawa, 2008), often interpreted as considering a uniform prior for the model parameters (Bhat & Kumar, 2010; Sodhi & Ehrlich, 2010). Though the uniform distribution on parameters may be viewed as a naturally uninformative, it is well known that model selection using the marginal likelihood assuming an uninformative prior specification can lead to selection of the simplest model independently of the data (see e.g. Jeffreys, 1998; Jennison, 1997; Lindley, 1957). As a result, while BIC can provide consistent selection of nested models, it can punish extra complexity in an excessive manner.

To illustrate this phenomenon we consider data generated from an HSMM with the same formulation as above except that in this scenario the dwell distribution is a negative-binomial parameterized by state specific parameters $\boldsymbol{\lambda} = (3.33, 2.50)$ and $\boldsymbol{\rho} = (2, 0.5)$. Note that the data generating HSMM has two more parameters than the HMM. For the HSMM approximation, we select $\mathbf{a} = (10, 10)$ thus providing negligible truncation of the right tail for the dwell distribution, given the data generating parameters. Figure 6 (bottom) shows box-plots of the difference between the model scores (marginal-likelihood and BIC) across 20 simulated time series when fitting the HMM and HSMM, for increasing sample size $T = 200, 1000, 5000$. We negate the BIC so that the preferred model maximises both criteria. Unlike the experiments described above, the data is now from the less parsimonious HSMM approach and therefore negative values for the difference in score corresponds to correctly selecting the more complicated model. For small samples sizes, e.g. $T = 200, 1000$, the complexity penalty of

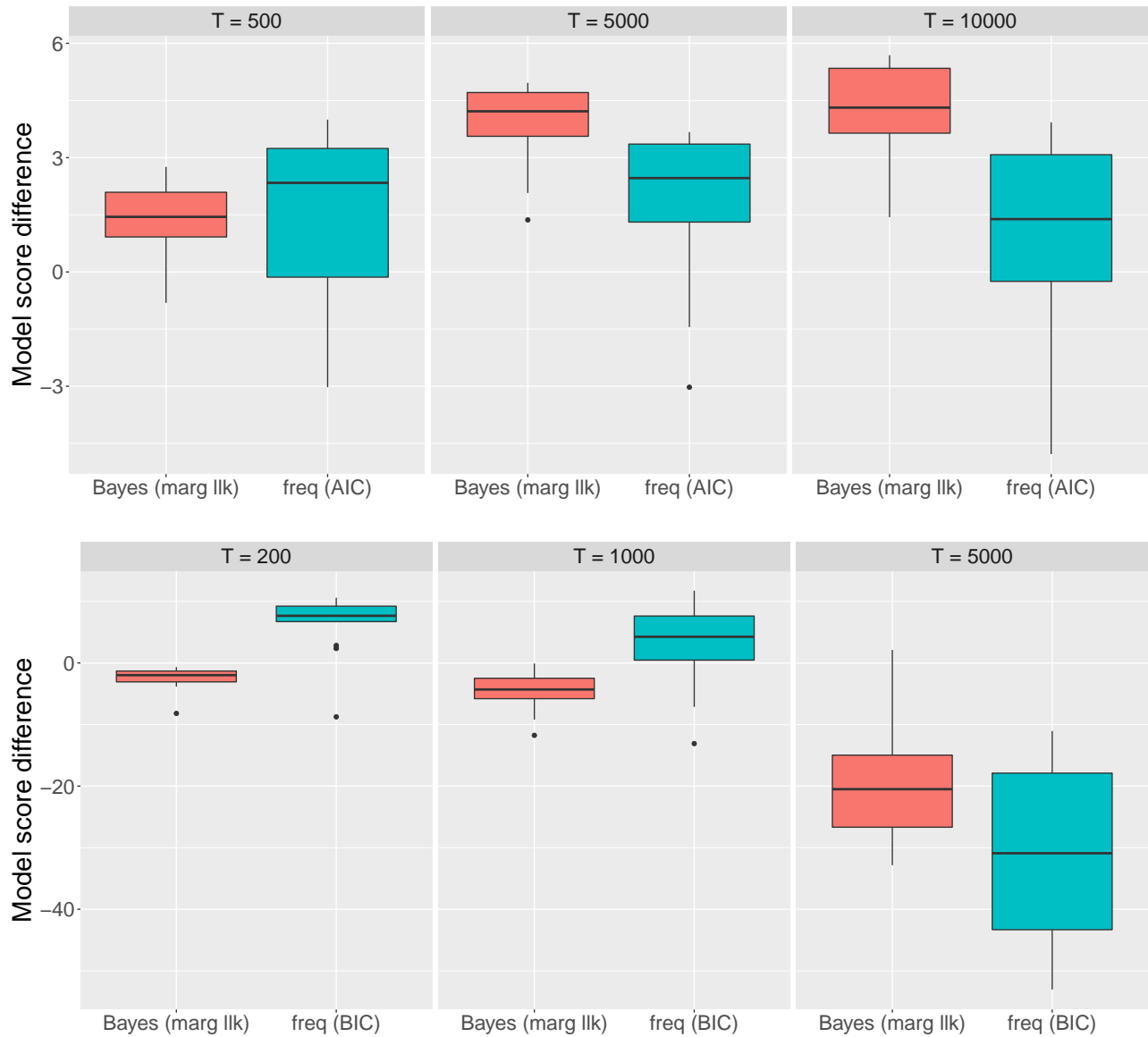


Figure 6: AIC, BIC and the marginal likelihood for nested models. (Top) model score differences between an unstructured start geometric tail duration HSMM with $\mathbf{a} = \mathbf{m} = (2, 2)$ and a HMM when the data is generated from the latter. Positive values of the model score difference correspond to correctly selecting the simpler model. The marginal likelihood provides consistent model selection as $T \rightarrow \infty$ where AIC does not. (Bottom) model score differences between a negative-binomial duration HSMM approximated by a threshold $\mathbf{a} = (10, 10)$ and a HMM when the data is generated from the former. Negative values of the model score difference correspond to correctly selecting the more complicated model. The marginal likelihood penalizes complexity less extremely than BIC.

the BIC appears to be too large, so that in almost all of the 20 repeat experiments the simple model is incorrectly favoured over the correct data generating model, i.e. the HSMM. On the other hand, the marginal likelihood is able to correctly select the more complicated model across almost all simulations and sample sizes. The supplementary material contains results of an additional experiment considering data from a negative binomial dwell distribution as well as full details of the prior specification.

Naturally, the results of this section are dependent upon the the prior specifications for the marginal likelihood. What we aim to demonstrate here are some of the drawbacks of using AIC and BIC for model selection and that, provided careful consideration is given to the prior specification, both large sample consistency and small sample efficiency can be achieved when following a Bayesian paradigm.

5 Telemetric Activity Data

We analyze the physical activity (PA) time series that was investigated using a frequentist HMM by [Huang et al. \(2018\)](#). We seek to conduct a similar study but within a Bayesian framework and considering the extra flexibility afforded by our proposed methodology to investigate departures from the HMM. In order to do so, three-state HSMMs with Poisson (λ_j) and Neg-Binomial (λ_j, ρ_j) dwell durations, shifted to have strictly non-negative support and approximated via a threshold $\mathbf{a} = (150, 10, 10)$, are fitted to the square root of the PA time series shown in [Figure 1](#), wherein we assume that transformed observations are generated from Normal(μ_j, σ_j^2) distributions, as in [Huang et al. \(2018\)](#). We specified $K = 3$ states, in agreement with findings of [Migueles et al. \(2017\)](#) and [Huang et al. \(2018\)](#), where they collected results from more than forty experiments on PA time series. In their studies, for each individual the lowest level of activity corresponds to the sleeping period, which usually happens during the night, while the other two phases are mostly associated with movements happening in the daytime. Hence, these different telemetric activities are represented as inactive (IA), moderately active (MA) and highly active (HA) states.

We assume that the night rest period of a healthy individual is generally between 7 and 8 hours. The parameter of the dwell duration of IA state, say λ_{IA} , is hence assigned a Gamma prior with hyperparameters that reflects mean 90 (i.e. $7.5 \cdot 12$) and variance 36 (i.e. $[0.5 \cdot 12]^2$), the latter chosen to account for some variability amongst people. Since usually we do not have significant prior knowledge on how long people might spend time in MA and HA states, we assigned λ_{MA} and λ_{HA} Gamma priors with mean 24 (i.e. 2 hours) and variance 324 (i.e. $[1.5 \cdot 12]^2$) to reflect high degree

of uncertainty. The approximation threshold was chosen as $\mathbf{a} = (150, 10, 10)$ to reflect a trade-off between accurately capturing the states with which we have considerable prior information, i.e. IA, whilst improving the computational efficiency of the other states over a standard HSMM formulation. Transition probabilities from state IA, say $\boldsymbol{\pi}_{\text{IA}}$, are specified as Dirichlet in such a way that there is equal prior probability of switching to any of the active states, i.e. MA or HA. On the other hand, active states usually alternate between each other more frequently than with IA (Huang et al., 2018), and thus we may set the hyperparameters for the prior probabilities $\boldsymbol{\pi}_{\text{MA}}$ so that transitions from MA to HA are four times more likely than switching from MA to IA (a similar argument can be made for $\boldsymbol{\pi}_{\text{HA}}$). Finally, priors for the inverse of dispersion parameters ρ_j^{-1} are specified as Gamma(2, 2), and for the Gaussian emissions are given as Normal(\bar{y} , 4) and Inverse-Gamma(2, 0.5) for locations μ_j and scale σ_j^2 , respectively, where \bar{y} denotes the sample mean.

For each proposed model our Bayesian procedure is run for 6,000 iterations, 1,000 of which are discarded as burn-in. Firstly, we consider selecting which of the competing dwell distributions, i.e. the geometric dwell characterising the HMM and the Poisson and negative binomial HSMM extensions, is most supported by the observed data. As explained in Section 3.3, we specified hyperparameters for these competing models so that the corresponding priors match means and variances of the informative prior specification given above. In order to measure the gain of including available prior knowledge into the model, we also investigated predictive performances when specifying a weakly informative prior setting (as in Section 4.1). Table 3 displays marginal likelihood for the different models and posterior means of the corresponding dwell parameters. It is clear that integrating into the model available prior information improves performance greatly. In addition, modelling dwell durations as either negative-binomial or geometric yields superior predictive results compared to a Poisson model. Furthermore, the Bayes factor 7.92 (i.e. $\exp\{-1633.25 + 1635.32\}$) suggests that there is *substantial evidence* (Kass & Raftery, 1995) in favour of the HSMM with negative binomial durations in comparison to a standard HMM. This is also reflected by the estimated posterior means of the parameters ρ_j which differ from one, hence showing some departure from geometric dwell durations. These ‘dispersion’ parameters are smaller than one for the IA and MA states indicating a larger fitted variance under the negative-binomial HSMM. Combined with their estimated means, it may explain the improved performance of the negative-binomial dwell model over the HMM. The increased variance allows the time series to better capture the short transitions to IA states seen in the fitted model (Figure 7). This also explains why the Poisson HSMM performs poorly for this dataset; the fitted Poisson dwell distribution

for the IA state can be seen to have a much smaller variance than the geometric and negative-binomial alternatives. Future work could consider more complex dwell distributions to reflect the different patterns of human sleep. For example, a natural extension to the results presented here could be to look at whether a two component mixture distribution (e.g. Poisson) can aid in better capturing the short excursions to the IA seen in Figure 7.

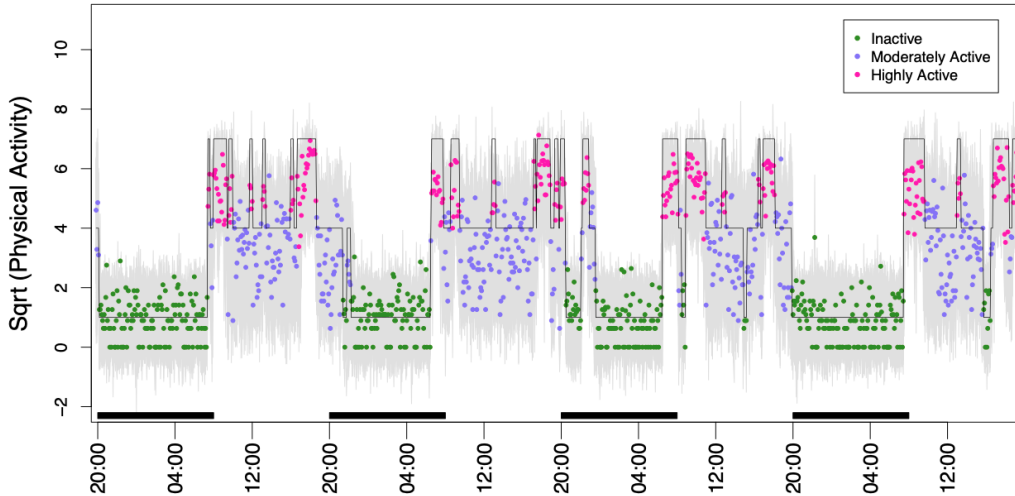


Figure 7: Square root of the PA time series along with simulated observations from our fitted model with negative-binomial dwell-time, where the piecewise horizontal line represents the estimated state sequence. Rectangles on the time axis correspond to periods from 20.00 to 8.00. IA state happens during night, whereas days are characterized by many switches between MA and HA states. This picture is best viewed in color.

Posterior means of the emission parameters were $y_t|_{IA} \sim \text{Normal}(0.93, 0.47)$, $y_t|_{MA} \sim \text{Normal}(3.17, 1.28)$ and $y_t|_{HA} \sim \text{Normal}(5.38, 0.54)$. We observe that IA state is characterized by low values and MA state shows larger variance than the other two telemetric patterns. Posterior means of dwell parameters are provided in Table 3, showing an average sleeping behavior of about 7 hours and a half, for this individual. In Figure 8, we display posterior histograms of the transition probabilities between different states. There seems to be high chances of switching between active states, since the posterior means for $\pi_{HA \rightarrow MA}$ and $\pi_{MA \rightarrow HA}$ are close to one, though the latter exhibiting large variance. Additionally, the posterior probability of transitioning from HA to IA is very close to zero, which is reasonable considering that it is very unlikely that, for instance, an individual would go to sleep

Table 3: Telemetric activity data. Marginal likelihood for different dwell durations (i.e. Poisson, geometric and negative-binomial), where the superscript \dagger denotes a weakly informative prior specification. Geometric durations are also being characterized by the mean dwell length $\lambda_j = 1/(1 - \gamma_{jj})$ where γ_{jj} represents the probability of self-transition. Estimated posterior means of the distinct dwell parameters are reported with a 95% credible intervals obtained from the posterior sample.

	marg llk	λ_{IA}	λ_{MA}	λ_{HA}	ρ_{IA}	ρ_{MA}	ρ_{HA}
Poisson \dagger	-1694.82	112.71 (104.42-119.75)	14.45 (13.28-15.61)	12.71 (9.95-12.71)	-	-	-
Geometric \dagger	-1649.95	45.93 (26.62-76.88)	10.52 (7.51-14.53)	8.60 (6.11-12.04)	-	-	-
Neg-Binom \dagger	-1646.82	45.96 (21.35-87.39)	11.05 (6.36-18.51)	8.24 (5.38-12.04)	0.51 (0.29-1.08)	0.52 (0.32-1.01)	0.93 (0.53-2.04)
Poisson	-1681.62	104.40 (97.69-111.20)	14.48 (13.34-15.61)	11.32 (9.92-12.79)	-	-	-
Geometric	-1635.32	88.79 (79.42-99.07)	13.33 (9.52-18.6)	11.01 (7.84-15.15)	-	-	-
Neg-Binom	-1633.25	89.01 (79.44-98.83)	12.87 (7.71-21.25)	9.07 (5.91-13.40)	0.66 (0.33-1.17)	0.68 (0.36-1.16)	1.11 (0.55-1.96)

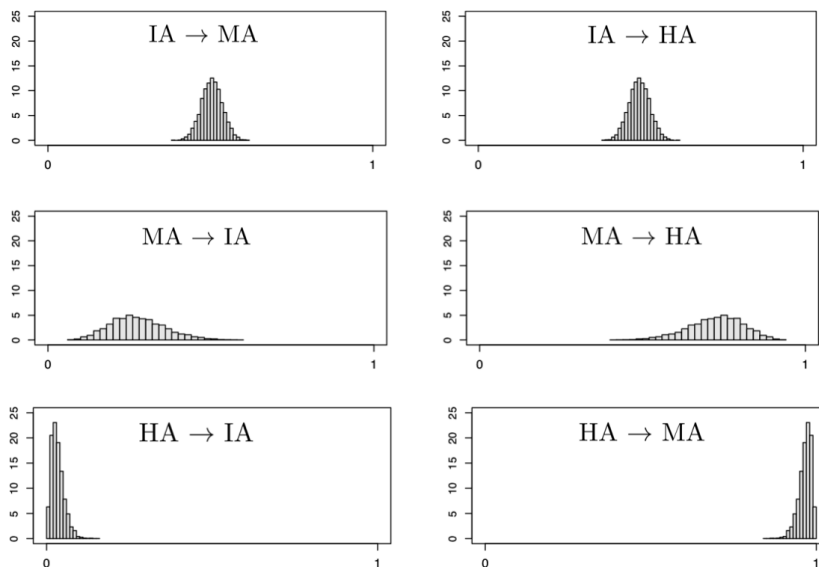


Figure 8: Estimated posterior density histograms of the transition probabilities between IA, MA, and HA states, where estimation was carried out using our proposed HSMM with negative binomial dwell-time.

straight after having performed intense physical activity. Figure 7 shows the transformed time series as well as simulated data from the predictive distribution, and the estimated hidden state sequence using the Viterbi algorithm. It can be seen that IA state occurs during night whereas days are characterized by many switches between MA and HA states. Our results are in agreement with [Huang et al. \(2018\)](#).

6 Concluding Summaries

We presented a Bayesian model for analyzing time series data based on the HSMM approximation introduced by [Langrock and Zucchini \(2011\)](#) in which a special structure of the transition matrix is embedded to model the state duration distributions. We showed the advantages of choosing a Bayesian paradigm over its frequentist counterpart in terms of incorporation of prior information, quantification of uncertainty, model selection and forecasting. The proposed approach allows for the development of highly flexible and interpretable models that incorporate available prior information on state durations. Our methodology is applied to physical activity data collected from a wearable sensing device, where we successfully described the probabilistic dynamics governing the transitions between different activity patterns during the day as well as characterizing the sleep duration over

night. Future work will address extending our methodology to multivariate time series as well as including covariates.

Supplementary Material

Supplementary materials are available and include further details about dwell-durations, forecasting function, graphs of normal pseudo-residuals and further experiments for nested models. Code that implements the methodology is available as online supplemental material and can be found at <https://github.com/Beniamino92/BayesianApproxHSMM>.

Acknowledgements

The authors would like to thank David Rossell for useful discussions about Bayesian model selection, AIC and BIC.

References

- Aitchison, J. (1975). Goodness of prediction fit. *Biometrika*, *62*(3), 547–554.
- Akaike, H. (1973). Information theory and an extension of the maximum likelihood principle. In *Second international symposium on information theory* (p. 267281).
- Ancoli-Israel, S., Cole, R., Alessi, C., Chambers, M., Moorcroft, W., & Pollak, C. P. (2003). The role of actigraphy in the study of sleep and circadian rhythms. *Sleep*, *26*(3), 342–392.
- Ancoli-Israel, S., Martin, J. L., Blackwell, T., Buenaiver, L., Liu, L., Meltzer, L. J., . . . Taylor, D. J. (2015). The SBSM guide to actigraphy monitoring: clinical and research applications. *Behavioral Sleep Medicine*, *13*(sup1), S4–S38.
- Aung, M. H., Matthews, M., & Choudhury, T. (2017). Sensing behavioral symptoms of mental health and delivering personalized interventions using mobile technologies. *Depression and Anxiety*, *34*(7), 603–609.
- Bhat, H. S., & Kumar, N. (2010). On the derivation of the Bayesian Information Criterion. *School of Natural Sciences, University of California*.

- Bulla, J., Bulla, I., & Nenadić, O. (2010). HSMMAAn R package for analyzing hidden semi-Markov models. *Computational Statistics & Data Analysis*, *54*(3), 611–619.
- Carpenter, B., Gelman, A., Hoffman, M., Lee, D., Goodrich, B., Betancourt, M., ... Riddell, A. (2016). Stan: A probabilistic programming language. *Journal of Statistical Software*, *20*.
- Cox, D. (2006). Frequentist and Bayesian statistics: A critique (Keynote address). In *Statistical problems in particle physics, astrophysics and cosmology* (pp. 3–6). World Scientific.
- Douglas, N. J., Thomas, S., & Jan, M. A. (1992). Clinical value of polysomnography. *The Lancet*, *339*(8789), 347–350.
- Duane, S., Kennedy, A. D., Pendleton, B. J., & Roweth, D. (1987). Hybrid Monte Carlo. *Physics Letters B*, *195*(2), 216–222.
- Forney, G. D. (1973). The Viterbi algorithm. *Proceedings of the IEEE*, *61*(3), 268–278.
- Fujikoshi, Y. (1985). Selection of variables in two-group discriminant analysis by error rate and Akaike’s information criteria. *Journal of Multivariate Analysis*, *17*(1), 27–37.
- Gelfand, A. E., & Smith, A. F. (1990). Sampling-based approaches to calculating marginal densities. *Journal of the American Statistical Association*, *85*(410), 398–409.
- Gelman, A., Carlin, J. B., Stern, H. S., Dunson, D. B., Vehtari, A., & Rubin, D. B. (2013). *Bayesian data analysis*. CRC press.
- Gelman, A., Hwang, J., & Vehtari, A. (2014). Understanding predictive information criteria for bayesian models. *Statistics and Computing*, *24*(6), 997–1016.
- Gelman, A., Simpson, D., & Betancourt, M. (2017). The prior can often only be understood in the context of the likelihood. *Entropy*, *19*(10), 555.
- Griewank, A., & Walther, A. (2008). *Evaluating derivatives: principles and techniques of algorithmic differentiation* (Vol. 105). SIAM.
- Gronau, Q., Singmann, H., & Wagenmakers, E.-J. (2020). Bridgesampling: An R package for estimating normalizing constants. *Journal of Statistical Software*, *92*(10).
- Guédon, Y. (2003). Estimating hidden semi-Markov chains from discrete sequences. *Journal of Computational and Graphical Statistics*, *12*(3), 604–639.
- Hadj-Amar, B., Finkenstädt, B., Fiecas, M., & Huckstepp, R. (2020). Identifying the Recurrence of Sleep Apnea Using a Spectral Hidden Markov Model. *arXiv preprint arXiv:2001.01676*.

- Hadj-Amar, B., Finkenstädt, B., Fiecas, M., Lévi, F., & Huckstepp, R. (2019). Bayesian Model Search for Nonstationary Periodic Time Series. *Journal of the American Statistical Association*, 1–29.
- Hoffman, M. D., & Gelman, A. (2014). The No-U-Turn sampler: adaptively setting path lengths in Hamiltonian Monte Carlo. *Journal of Machine Learning Research*, 15(1), 1593–1623.
- Huang, Q., Cohen, D., Komarzynski, S., Li, X.-M., Innominato, P., Lévi, F., & Finkenstädt, B. (2018). Hidden Markov models for monitoring circadian rhythmicity in telemetric activity data. *Journal of The Royal Society Interface*, 15(139), 20170885.
- Jeffreys, H. (1998). *The theory of probability*. OUP Oxford.
- Jelinek, F. (1997). *Statistical methods for speech recognition*. MIT press.
- Jennison, C. (1997). Discussion of “On Bayesian analysis of mixtures with an unknown number of components” by S. Richardson and P.J. Green. *Journal of the Royal Statistical Society: Series B (Statistical Methodology)*, 59(4), 778–779.
- Jewson, J., Smith, J., & Holmes, C. (2018). Principles of Bayesian inference using general divergence criteria. *Entropy*, 20(6), 442.
- Johnson, M. J., & Willsky, A. S. (2013). Bayesian nonparametric hidden semi-Markov models. *Journal of Machine Learning Research*, 14(Feb), 673–701.
- Kass, R. E., & Raftery, A. E. (1995). Bayes factors. *Journal of the American Statistical Association*, 90(430), 773–795.
- Kaur, G., Phillips, C., Wong, K., & Saini, B. (2013). Timing is important in medication administration: a timely review of chronotherapy research. *International Journal of Clinical Pharmacy*, 35(3), 344–358.
- Konishi, S., & Kitagawa, G. (2008). *Information criteria and statistical modeling*. Springer Science & Business Media.
- Langrock, R., Swihart, B. J., Caffo, B. S., Punjabi, N. M., & Crainiceanu, C. M. (2013). Combining hidden Markov models for comparing the dynamics of multiple sleep electroencephalograms. *Statistics in Medicine*, 32(19), 3342–3356.
- Langrock, R., & Zucchini, W. (2011). Hidden Markov models with arbitrary state dwell-time distributions. *Computational Statistics & Data Analysis*, 55(1), 715–724.

- Leroux, B. G., & Puterman, M. L. (1992). Maximum-penalized-likelihood estimation for independent and Markov-dependent mixture models. *Biometrics*, 545–558.
- Lindley, D. V. (1957). A statistical paradox. *Biometrika*, 44(1/2), 187–192.
- Meng, X.-L., & Schilling, S. (2002). Warp bridge sampling. *Journal of Computational and Graphical Statistics*, 11(3), 552–586.
- Meng, X.-L., & Wong, W. H. (1996). Simulating ratios of normalizing constants via a simple identity: a theoretical exploration. *Statistica Sinica*, 831–860.
- Migueles, J. H., Cadenas-Sanchez, C., Ekelund, U., Nyström, C. D., Mora-Gonzalez, J., Löf, M., . . . Ortega, F. B. (2017). Accelerometer data collection and processing criteria to assess physical activity and other outcomes: a systematic review and practical considerations. *Sports Medicine*, 47(9), 1821–1845.
- Neal, R. M., et al. (2011). MCMC using Hamiltonian dynamics. *Handbook of Markov chain Monte Carlo*, 2(11), 2.
- O’Hagan, A., & Forster, J. J. (2004). *Kendall’s advanced theory of statistics, volume 2B: Bayesian inference* (Vol. 2). Arnold.
- Rabiner, L. R. (1989). A tutorial on hidden Markov models and selected applications in speech recognition. *Proceedings of the IEEE*, 77(2), 257–286.
- Rabiner, L. R., Wilpon, J. G., & Soong, F. K. (1989). High performance connected digit recognition using hidden Markov models. *IEEE Transactions on Acoustics, Speech, and Signal Processing*, 37(8), 1214–1225.
- Raviv, J. (1967). Decision making in Markov chains applied to the problem of pattern recognition. *IEEE Transactions on Information Theory*, 13(4), 536–551.
- Robert, C. (2007). *The Bayesian choice: from decision-theoretic foundations to computational implementation*. Springer Science & Business Media.
- Sadeh, A. (2011). The role and validity of actigraphy in sleep medicine: an update. *Sleep Medicine Reviews*, 15(4), 259–267.
- Sansom, J., & Thomson, P. (2001). Fitting hidden semi-Markov models to breakpoint rainfall data. *Journal of Applied Probability*, 38(A), 142–157.

- Schwarz, G., et al. (1978). Estimating the dimension of a model. *The Annals of Statistics*, 6(2), 461–464.
- Silva, B. M., Rodrigues, J. J., de la Torre Díez, I., López-Coronado, M., & Saleem, K. (2015). Mobile-health: A review of current state in 2015. *Journal of Biomedical Informatics*, 56, 265–272.
- Sodhi, N. S., & Ehrlich, P. R. (2010). *Conservation biology for all*. Oxford University Press.
- Spiegelhalter, D. J., Best, N. G., Carlin, B. P., & Van Der Linde, A. (2002). Bayesian measures of model complexity and fit. *Journal of the Royal Statistical Society: Series B (Statistical Methodology)*, 64(4), 583–639.
- Stan Development Team. (2018). *Stan functions reference* (Vol. 2.23). Retrieved from <https://mc-stan.org/docs/2.23/functions-reference/index.html>
- Stephens, M. (2000). Dealing with label switching in mixture models. *Journal of the Royal Statistical Society: Series B (Statistical Methodology)*, 62(4), 795–809.
- Watanabe, S. (2010). Asymptotic equivalence of bayes cross validation and widely applicable information criterion in singular learning theory. *Journal of Machine Learning Research*, 11(Dec), 3571–3594.
- Williams, J., Roth, A., Vathauer, K., & McCrae, C. S. (2013). Cognitive behavioral treatment of insomnia. *Chest*, 143(2), 554–565.
- Zucchini, W., MacDonald, I. L., & Langrock, R. (2017). *Hidden Markov models for time series: an introduction using R*. CRC press.